This article was downloaded by: [University of Haifa Library]
On: 09 August 2012, At: 14:55
Publisher: Taylor & Francis
Informa Ltd Registered in England and Wales Registered Number: 1072954
Registered office: Mortimer House, 37-41 Mortimer Street, London W1T 3JH, UK

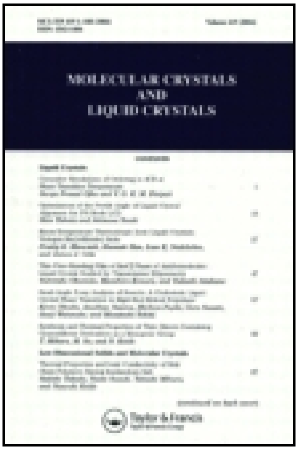

Molecular Crystals and Liquid Crystals
Publication details, including instructions for authors and subscription information:
http://www.tandfonline.com/loi/gmcl20

Molecular Direction Dependence of Shear Horizontal Wave Propagation in Nematic Liquid Crystal

Ryotaro Ozaki [a], Masashi Aoki [a], Hiroshi Moritake [a], Katsumi Yoshino [b] & Kohji Toda [c]

[a] Department of Electrical and Electronic Engineering, National Defense Academy, Yokosuka, Kanagawa, Japan

[b] Research Project Promotion Institute, Shimane University, Matsue, Shimane, Japan

[c] Mechanical System Engineering, Faculty of Engineering, Musashi Institute of Technology, Setagaya-ku, Tokyo, Japan

Version of record first published: 22 Sep 2010

To cite this article: Ryotaro Ozaki, Masashi Aoki, Hiroshi Moritake, Katsumi Yoshino & Kohji Toda (2007): Molecular Direction Dependence of Shear Horizontal Wave Propagation in Nematic Liquid Crystal, Molecular Crystals and Liquid Crystals, 477:1, 101/[595]-112/[606]

To link to this article: http://dx.doi.org/10.1080/15421400701686710

PLEASE SCROLL DOWN FOR ARTICLE

Full terms and conditions of use: http://www.tandfonline.com/page/terms-and-conditions

This article may be used for research, teaching, and private study purposes. Any substantial or systematic reproduction, redistribution, reselling, loan, sub-licensing, systematic supply, or distribution in any form to anyone is expressly forbidden.

The publisher does not give any warranty express or implied or make any representation that the contents will be complete or accurate or up to date. The accuracy of any instructions, formulae, and drug doses should be independently verified with primary sources. The publisher shall not be liable for any loss, actions, claims, proceedings, demand, or costs or damages whatsoever or howsoever caused arising directly or indirectly in connection with or arising out of the use of this material.

Downloaded by [University of Haifa Library] at 14:55 09 August 2012

Mol. Cryst. Liq. Cryst., Vol. 477, pp. 101/[595]–112/[606], 2007
Copyright © Taylor & Francis Group, LLC
ISSN: 1542-1406 print/1563-5287 online
DOI: 10.1080/15421400701686710

Downloaded by [University of Haifa Library] at 14:55 09 August 2012

Molecular Direction Dependence of Shear Horizontal Wave Propagation in Nematic Liquid Crystal

Ryotaro Ozaki
Masashi Aoki
Hiroshi Moritake
Department of Electrical and Electronic Engineering, National Defense Academy, Yokosuka, Kanagawa, Japan

Katsumi Yoshino
Research Project Promotion Institute, Shimane University, Matsue, Shimane, Japan

Kohji Toda
Mechanical System Engineering, Faculty of Engineering, Musashi Institute of Technology, Setagaya-ku, Tokyo, Japan

The acoustic phase of a shear horizontal (SH) wave propagating into a nematic liquid crystal cell is measured. To investigate the acoustic phase depending on the director angle of a liquid crystal, the two SH wave devices having different initial molecular orientations are fabricated. The acoustic phase change of the SH wave devices is measured for various applied electric fields. The numerical analyses are also performed by considering director distribution in the nematic liquid crystal layer. The experimental acoustic phase changes are well accorded with the calculated shear stresses as a viscous resistance.

Keywords: nematic liquid crystal; shear stress; ultrasonic wave; viscosity

INTRODUCTION

Liquid crystal having anisotropies of dielectric constant, refractive index, and viscosity is a vital material for functional applications. The anisotropy based on a cylindrical molecular shape is easily

Address correspondence to Ryotaro Ozaki, Department of Electrical and Electronic Engineering, National Defense Academy, #1-10-20# Hashirimizu, Yokosuka, Kanagawa #239-8686, Japan. E-mail: ozaki@nda.ac.jp

controllable by reorientation of the molecules upon application of electric field. Almost all of the applications of liquid crystals are usually used in a cell structure. Since the anisotropies depend on a director distribution of liquid crystal, a measurement of the director distribution in the cell structure is useful for developing and design of applications. The behavior of the liquid crystal director in the vicinity of the substrate surface has been investigated by several optical methods [1–3].

On the other hand, acoustic wave devices have attracted considerable interest in a field of liquid environments [4–6]. As typical example of using acoustics, dynamic visoelastic properties of nematic liquid crystals have been investigated using a quartz crystal resonator [7]. A surface acoustic wave device is also applied to measure viscosity of liquids. Although the devices require low energy loss for liquid sensing, Rayleigh and Lamb wave devices immersed in viscous fluid have high propagation loss at the solid/liquid interface because of radiation into the liquid medium in the form of a longitudinal wave [8,9]. A use of a shear horizontal (SH) wave is considered to be favorable for investigating liquid properties because the SH wave does not suffer from propagation loss at the solid/liquid interface. Recently, we have proposed a method for measuring the liquid crystal viscosity in the vicinity of the substrate surface using SH wave [10–15].

In this study, the acoustic phase of the SH wave propagating in a liquid crystal cell is measured. Two SH wave devices having different initial molecular alignments in the liquid crystal cell has fabricated. The numerical analysis of the displacement distribution of SH wave is performed by using hydrodynamics and continuum physics. The shear stresses in the liquid crystal layer are also calculated considering the viscosity distribution as a function of electric field. The experimental acoustic phase changes are compared with the calculated shear stresses as a viscous resistance.

EXPERIMENTAL PROCEDURES

Figure 1 shows the schematic construction of the SH devices having a liquid crystal cell. The liquid crystal layer, located on the center of the acoustic delay line, was sandwiched between two glass plates coated with In-Sn oxide (ITO). We prepared the two devices having a different molecular alignment to investigate the acoustic phase depending on the director angle. The initial orientations of the Devices 1 and 2 were along the y- and the x-axes, as shown in Figure 1. The tested liquid crystal sample was 4-cyano-4′-pentylbiphenyl (5CB) with a positive dielectric anisotropy. The surfaces of the glass plates were coated with polyimide (JSR, AL1254) and rubbed in one direction for

Downloaded by [University of Haifa Library] at 14:55 09 August 2012

Downloaded by [University of Haifa Library] at 14:55 09 August 2012

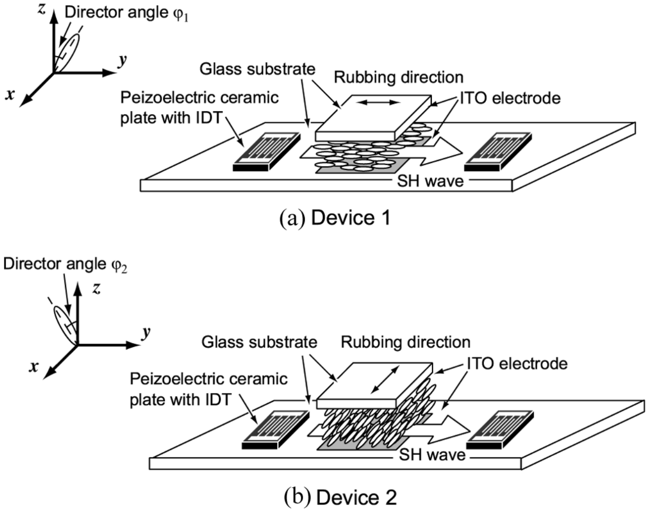

FIGURE 1 Schematic construction of the SH wave device used in this study.

unidirectional alignment. The thickness of the liquid crystal layer was adjusted by polyethylene-terephthalate films of 32 μm as a spacer. Two 1-mm-thick piezoelectric ceramic plates (TDK, 101 A) having the poling axis parallel to the x-axis, were cemented at both ends on the upper surface of a 400-μm-thick glass plate (Corning, 7059). Two interdigital transducers (IDTs) with an interdigital periodicity of 400 μm and 7 electrode-finger pairs were evaporated on each of the piezoelectric ceramic plates.

Figure 2 shows the experimental setup for measurement of the acoustic phase change. One IDT was used for exciting the SH wave and the other IDT was for receiving. A sine voltage with frequency

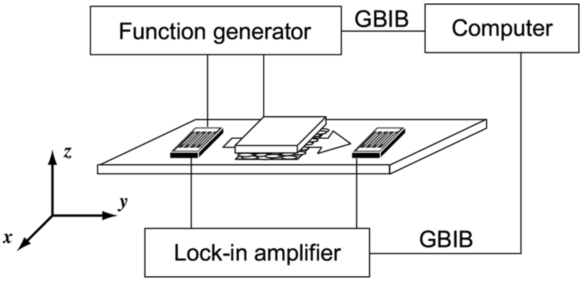

FIGURE 2 Measurement setup for acoustic phase of the SH wave propagating in liquid crystal cell.

of 9 MHz was applied for SH wave excitation using a function generator with dual channels (Tektronix, AFG320). The SH wave propagates along the y-axis and the vibration direction of the SH wave is along the x-axis. The acoustic phase of the SH wave propagating in the cell structure was measured using an RF lock-in amplifier (Stanford Research Systems, SR844). On the other hand, an electric field was applied to the liquid crystal layer between two glass plates for control the molecular alignment. We define the director angle φ as the angle from the z-axis as shown in Figure 1. The applied voltage to the liquid crystal layer was a rectangular voltage with frequency of 2 kHz from the function generator (Tektronix, AFG320) and a power amplifier (NF, 4010).

Downloaded by [University of Haifa Library] at 14:55 09 August 2012

ANALYSIS PROCEDURES

The analysis of the SH wave propagation in the liquid crystal cell was performed by using hydrodynamics and continuum physics. When the viscous fluid is in contact with to the surface of the SH wave propagating medium, the acoustic phase delay arises due to the shear stress as a viscous resistance. This shear stress T in the viscous fluid is expressed by

$$T = \eta \frac{du}{dz}, \tag{1}$$

where η is a dynamic viscosity and u is a particle velocity in the viscous fluid.

In our device structure, the top surface of the lower glass plate is attached to the liquid crystal as viscous fluid. The SH wave displacement penetrates in the liquid crystal layer and the phase velocity slightly changes by the existence of the shear stress working as a friction force.

Since liquid crystals have a large anisotropy of viscosity depending on molecular alignment, it is important to consider the molecular director distribution in the liquid crystal layer. In this study, the molecular alignment was calculated based on the Franck continuum theory where the liquid crystal was regarded as an elastic continuum, and a free energy was taken into account both kinetic and electric energies. The free energy density g of a splay transition in the liquid crystal cell is determined by kinetic coefficients K_{11}, K_{33}, director vector $\boldsymbol{n}$ and electric field $\boldsymbol{E}$. Using the director angle φ the free energy density g is given by

$$g = \frac{1}{2}\left\{(K_{11}\cos^2\varphi + K_{33}\sin^2\varphi)\left(\frac{d\varphi}{dz}\right) - \varepsilon_0\varepsilon_a E^2 \sin^2\varphi\right\}, \tag{2}$$

where ε_0 is a dielectric constant of vacuum and ε_a is a dielectric anisotropy. The derivative of director angle φ can be determined by the

Downloaded by [University of Haifa Library] at 14:55 09 August 2012

Euler-Lagrange equation, and the director distribution is obtained by solving the differential equation of the director angle φ. The nematic liquid crystal has the viscosity anisotropy, where the viscosities of the Device 1 and 2 are defined to be η_1 and η_2, respectively. The dynamic viscosities η_1 and η_2 related director angle φ is expressed by

$$\eta_1 = \nu_3 \sin^2 \varphi + \nu_2 \cos^2 \varphi \tag{3}$$

$$\eta_2 = \nu_3 + 2(\nu_1 + \nu_2 - 2\nu_3) \sin^2 \varphi \cos^2 \varphi, \tag{4}$$

respectively, where ν_1, ν_2 and ν_3 are the MPP viscosity coefficients. The coefficients ν_1, ν_2 and ν_3 of 5CB are 0.024, 0.035 and 0.048 Pa · s [16].

The particle velocity in the liquid crystal layer was also calculated based on the Navier-Stokes equation as follows:

$$\frac{\partial u}{\partial t} = \frac{\eta}{\rho} \frac{\partial^2 u}{\partial x^2}, \tag{5}$$

where ρ is a density of the liquid crystal. We could obtain the shear stress linked with the acoustic phase change from Eq. (1) that is the product of the viscosity and the particle velocity derivative.

RESULTS AND DISCUSSION

Figure 3 shows the director angle dependence of the viscosities η_1 and η_2 expressed by Eqs. (3) and (4). The η_1 in the Device 1 decreases with

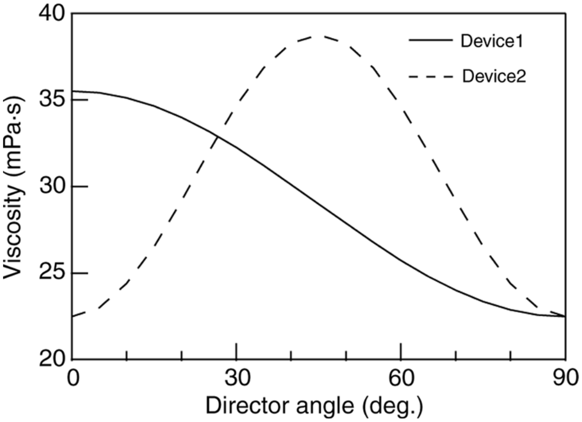

FIGURE 3 Director angle dependences of the viscosities of nematic liquid crystals having different molecular alignments.

Downloaded by [University of Haifa Library] at 14:55 09 August 2012

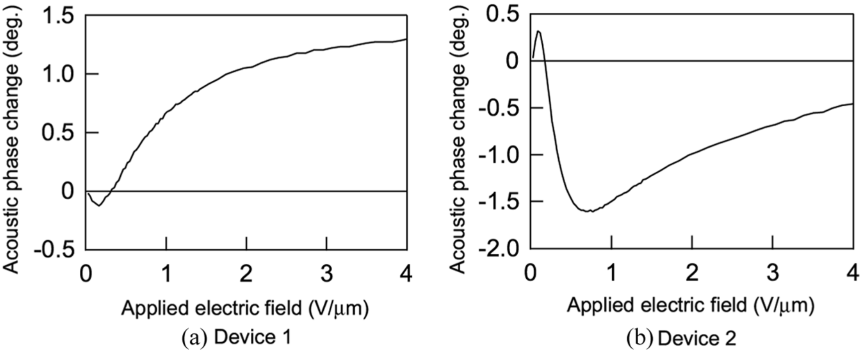

FIGURE 4 Measured applied electric field dependences of acoustic phase change of SH wave propagating in liquid crystal cells having different molecular alignment. (a) Molecular directors reorient from the y-axis to the z-axis. (b) Molecular directors from the x-axis to the z-axis.

increasing the director angle, while the η_2 in the Device 2 has a peak value. Although the initial viscosity at 0° is different between η_1 and η_2, they show the same value at 90°.

Figure 4 shows the measured applied electric field dependences of the acoustic phase change of SH wave propagating in the glass substrate. The acoustic phase changes were determined from the difference from the phase at 0 V as criterion. The acoustic phase change of the Device 1 is shown in Figure 4(a). The acoustic phase change decreased in the low electric fields and then increased with increasing applied electric field. The behavior at higher electric fields indicates that the acoustic phase advances with liquid crystal molecular reorientation. Since the viscosity in the Device 1 decreases with increasing the director angle φ by applying electric field, the viscous resistance also decreases for the propagation of SH wave. Therefore, the reduction of the viscous resistance produces the acoustic phase advance. However this viscosity change can not explain the phase delay at lower electric fields, because the viscosity has maximum at 0° as shown in Figure 3. On the other hand, Figure 4(b) shows the acoustic phase change in the Device 2. The acoustic phase change increased in the low electric fields and then decreased with increasing applied electric field via the peak value. The acoustic phase change increased again beyond the applied electric field of 0.7 V/μm. This curve approximately corresponded to the viscosity change in the Device 2 as shown in Figure 3. Therefore we could explain the acoustic phase change above 0.3 V/μm by using the viscosity change in the Device 2. But the acoustic phase

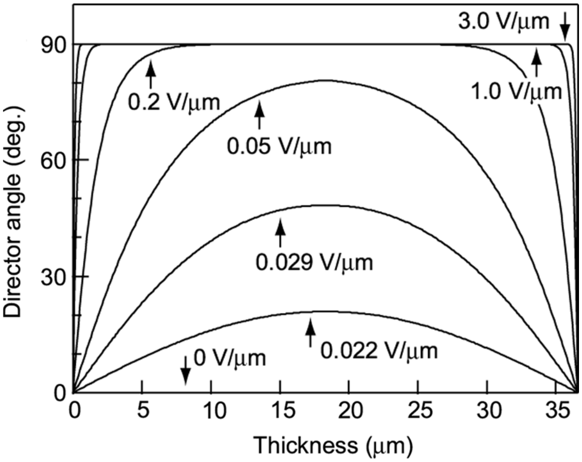

FIGURE 5 Director angle distributions in a 36-μm-thick cell as a function of applied electric field.

Downloaded by [University of Haifa Library] at 14:55 09 August 2012

change at low electric fields can not also explain by using the viscosity change of the liquid crystal layer.

For more detail investigation of the acoustic phase change with the liquid crystal molecular reorientation, the molecular director linked with the viscosity was calculated based on the Franck continuum theory. Figure 5 shows the calculated molecular director angle φ in the Device 1 having 36-μm-thickness, as a function of applied electric field. The 5CB having a positive anisotropy was used as the tested sample. The dielectric anisotropy ε_a is 10.5, and the elastic constants K_{11} and K_{33} are 6.4 and 10 pN, respectively. Under this condition, the Freedericksz threshold electric field E_c of the 36-μm-thick cell is about 0.02 V/μm. The liquid crystal molecules begin to move at E_c, and the molecules located at the center of the cell reorient dramatically above E_c. The boundary condition was assumed to be the strong anchoring because the liquid crystal molecules on the surface of the polyimide coated on the glass substrate were clamped due to the strong binding force. Thus, the director angles on both interfaces are 0° independently on the applied electric field, and the molecular alignment expands on an arched line with the increase of applied voltage, as shown in Figure 5. For the applied electric field beyond 3.0 V/μm, almost all of molecules reorient along the z-axis.

The viscosity distributions were determined by substituting the calculated director angles for Eqs. (3) or (4). Figure 6 shows the viscosity

Downloaded by [University of Haifa Library] at 14:55 09 August 2012

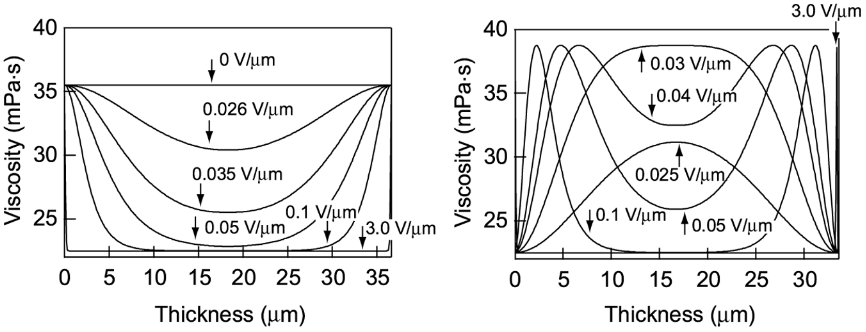

(a) Device 1 (b) Device 2

FIGURE 6 Viscosity distributions in the liquid crystal layer for various applied electric fields. (a) Viscosity distributions of the Device 1 in which molecular directors reorient from the y-axis to the z-axis. (b) Viscosity distributions of the Device 2 in which molecular directors from the x-axis to the z-axis.

distributions in the liquid crystal cells of the SH devices for various applied electric fields. The viscosity of the Device 1, that calculated by using Eq. (3), is shown in Figure 6(a). The viscosity distribution is constant at 0 V, because all of liquid crystal molecules are oriented along the y-axis. Above the E_c, the viscosity distribution changes with the reorientation of the molecules. The reorientation starting at center of the liquid crystal layer as shown in Figure 4 leads to the decreasing viscosity, because the increment of the director angle φ produces the decrement of the viscosity as shown in Figure 3. Figure 6(b) shows the viscosity distribution change of the Device 2 as a function of applied electric field. These were obtained by substituting the director angles φ of the Device 2 for Eq. (4). Since the viscosity decreases and increases as shown in Figure 3, the viscosity distribution change of the Device 2 is more complex than that of the Device 1. First, the viscosity reaches at the highest value in the center, because the viscosity has the maximum at 45°. For the director angle beyond 45°, the viscosity in the center decreases, and the higher viscosity region shifts from the center to the both interfaces. Furthermore, the high viscosity regions become narrower with the application of higher voltage, because the almost all of molecules reorient along the z-axis.

The viscous resistance produces the acoustic phase change for the SH wave propagation. That is, the viscosity works as a friction force for SH wave oscillation. The friction appears as shear stress in the viscous fluid. If the viscous resistance does not work for acoustic wave propagation, this means that a fluid on the propagation medium are

Downloaded by [University of Haifa Library] at 14:55 09 August 2012

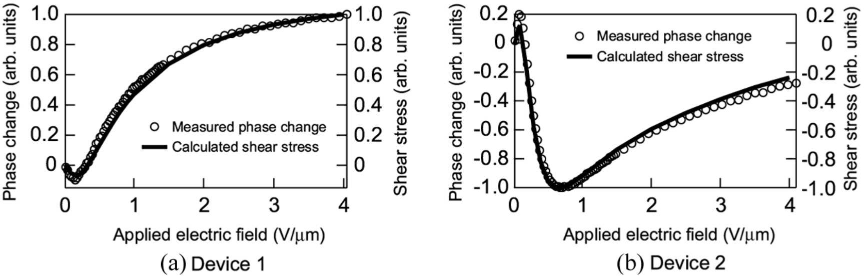

FIGURE 7 Measured acoustic phase change of SH wave and the shear stress calculated using the estimated viscosity.

an ideal fluid. But nematic liquid crystals are generally dealt with viscous fluids. Therefore, the analysis of the shear stress in the liquid crystal is needed for investigation of the viscous resistance linked with the acoustic phase. The shear stress in the liquid crystal layer was calculated from Eq. (1). The equation requires the viscosity and the space derivative of the particle velocity. The particle velocity in the liquid crystal cell was calculated based on the Navier-Stokes equation. In order to investigate the total viscous resistance working to the SH wave propagation, the shear stress was integrated over the liquid crystal layer thickness. When the viscosity used in the calculations was the 0.18 times as large as the viscosity measured in kHz region [16], the calculated shear stress curve well accorded with the measured acoustic phase change. Figure 7 shows the integration of shear stress over the liquid crystal layer using the estimated viscosity and the measured acoustic phase change $\Delta\theta$. It should be noted that the peak of the shear stress in the low electric fields also well agree with the measured acoustic phase change in both devices. These results indicate that the shear stress change in the liquid crystal corresponds to the acoustic phase change, and that the acoustic phase change is strongly related with the liquid crystal alignment. On the other hand, the reason of using the estimated viscosity is considered that the reference values are measured in kHz region but the frequency of SH wave in this study is 9 MHz. Details are now under study.

The characteristics of the acoustic phase changes can be explained by considering the distributions of the derivative of particle velocity and the viscosity. Figure 8 shows the derivative of particle velocity and the effective viscosity distributions in the Device 1 for various applied electric fields. The broken and solid lines are for the effective viscosity and for the derivative of the particle velocity, respectively. The acoustic phase changes were determined by a change from the phase at 0 V as criterion. In Figure 8(b), although the viscosity

Downloaded by [University of Haifa Library] at 14:55 09 August 2012

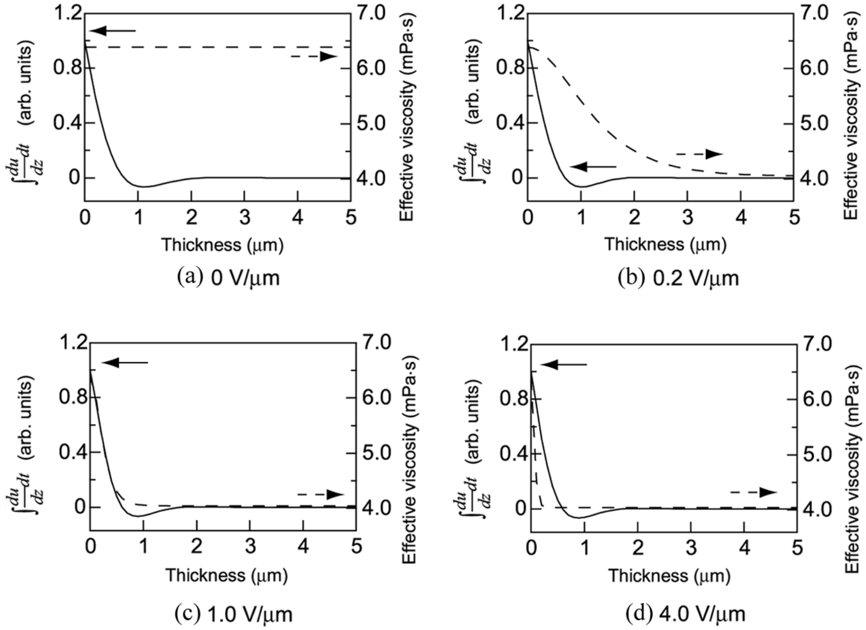

FIGURE 8 Viscosity distributions and derivatives of particle velocity in the Device 1 for various applied electric fields.

decreases from center of the cell, the derivative of particle velocity does not almost change. Because that is mainly governed by a frequency of SH wave. It should be noted that the viscosity decreases in the negative region of the derivative of particle velocity in Figure 8(b). This decrement produces the relative increment of the shear stress working as viscous resistance at the interface of the glass substrate. That is, the shear stress working as viscous resistance for SH wave propagation becomes large. This increment of viscous resistance results in the acoustic phase delay at low electric fields, as shown in Figure 7(a). Above the applied electric field of 0.2 V/μm, the viscosity decreases gradually with increasing applied voltage as shown in Figures 8(c) and (d). Therefore the viscous resistance also decreases and the acoustic phase advances as shown in Figure 7(a).

On the other hand, Figure 9 shows the derivative of particle velocity and the effective viscosity distributions in the Device 2 for various applied electric fields. The broken and solid lines are for the effective viscosity and for the derivative of the particle velocity, respectively. The characteristics of the acoustic phase changes of the Device 2 can also be explained by considering the distributions of the derivative

Downloaded by [University of Haifa Library] at 14:55 09 August 2012

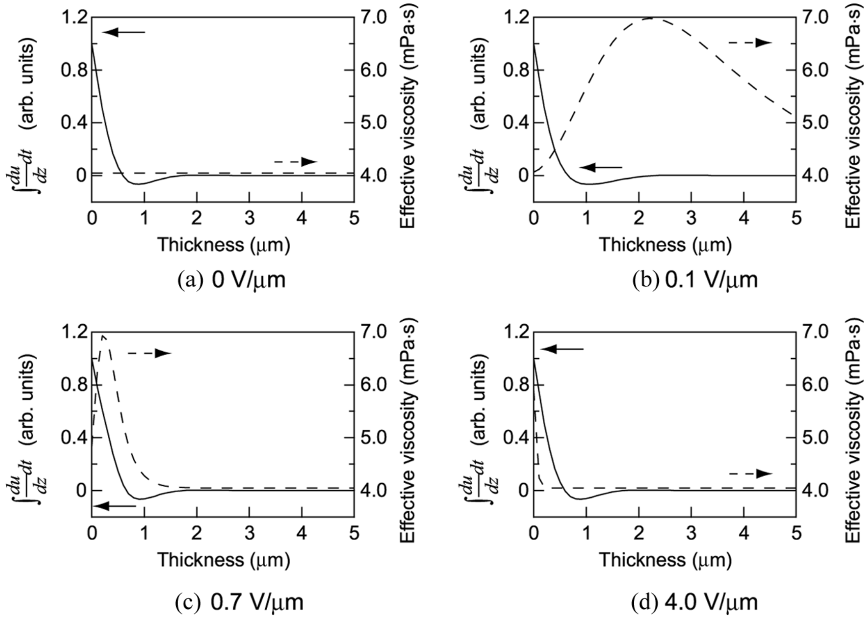

(a) 0 V/μm

(b) 0.1 V/μm

(c) 0.7 V/μm

(d) 4.0 V/μm

FIGURE 9 Viscosity distributions and derivatives of particle velocity in the Device 2 for various applied electric fields.

of particle velocity and the viscosity. As already mentioned, the high viscosity region shifts from the center of the cell to the both interfaces of the glass substrate as shown in Figure 6(b). In Figure 9(b), the higher viscosity is at the negative of the derivative of the particle velocity. The shear stress opposite side of the substrate interface becomes large. This result produces that the shear stress working as viscous resistance for SH wave propagation becomes small. Therefore, the acoustic phase slightly advances at 0.1 V/μm as shown in Figure 7(b). Above applied electric field of 0.1 V/μm, the acoustic phase change rapidly becomes negative with increasing the applied electric field. The phase delay shows the largest value for application of 0.7 V/μm because the high viscosity region matches to the positive region of the derivative of the particle velocity. The higher electric field, the acoustic phase advances again because the high viscosity region is narrower due to the molecules are reoriented along the z-axis, as shown in Figure 9(d).

CONCLUSIONS

The neatic liquid crystal director orientation in the vicinity of the glass plate was investigated in relation to the acoustic phase change of the shear horizontal (SH) wave propagating in a cell structure. The acoustic phases in two SH wave devices having different initial orientations were measured. The shear stress loading on the glass/liquid-crystal interface was calculated considering the distribution profiles of the liquid crystal molecules. The measured acoustic phase changes could be explained by with the calculated shear stress as viscous resistance. The acoustic phase change accompanied by the SH wave propagation was governed by the viscosity distributions and the particle velocities in the vicinity of the glass/liquid-crystal interface.

REFERENCES

[1] Yokoyama, H. & van Sprang, H. A. (1985). *J. Appl. Phys.*, *57*, 4520.

[2] Okutani, S., Kimura, M., & Akahane, T. (1998). *Jpn. J. Appl. Phys.*, *37*, L600.

[3] Okutani, S., Kimura, M., Toriumi, H., Akao, K., Tadokoro, T., & Akahane, T. (2001). *Jpn. J. Appl. Phys.*, *40*, 244.

[4] Castaings, M. & Cawley, P. (1996). *J. Acoust. Soc. Am.*, *100*, 3070.

[5] Bender, F., Dahint, R., & Josse, F. (1999). *IEEE Trans. Ultrason. Ferroelectr. Freq. Control*, *46*, 1497.

[6] Lucklum, R., Behling, C., & Hauptmann, P. (2000). *IEEE Trans. Ultrason. Ferroelectr. Freq. Control*, *47*, 216.

[7] Muramatsu, H. & Iwasaki, F. (1995). *Mol. Cryst. Liq. Cryst.*, *258*, 153.

[8] Sawaguchi, A. & Toda, K. (1992). *Jpn. J. Appl. Phys.*, *31*, 3094.

[9] Josse, F. & Shana, Z. (1989). *J. Acoust. Soc. Am.*, *85*, 1556.

[10] Inoue, M., Moritake, H., Toda, K., & Yoshino, K. (2000). *Jpn. J. Appl. Phys.*, *39*, 5632.

[11] Inoue, M., Yoshino, K., Moritake, H., & Toda, K. (2001). *Jpn. J. Appl. Phys.*, *40*, 3528.

[12] Inoue, M., Yoshino, K., Moritake, H., & Toda, K. (2002). *J. Appl. Phys.*, *91*, 2798.

[13] Moritake, H., Kim, J., Yoshino, K., & Toda, K. (2004). *Jpn. J. Appl. Phys.*, *43*, 6780.

[14] Moritake, H., Kim, J., Yoshino, K., & Toda, K. (2005). *Jpn. J. Appl. Phys.*, *44*, 4316.

[15] Ozaki, R., Aoki, M., Moritake, H., Yoshino, K., & Toda, K. (2006). *Jpn. J. Appl. Phys.*, *45*, 4662.

[16] Negita, K. (1996). *J. Chem. Phys.*, *105*, 7387.

Downloaded by [University of Haifa Library] at 14:55 09 August 2012